DOI: 10.61782/fa.2025.0297

FORUM ACUSTICUM
EURONOISE 2025

DG-TREFFTZ METHOD WITH RADIATING BOUNDARY CONDITIONS IMPOSED VIA THE NTD MAP: ANALYSIS ON A WAVEGUIDE

Peter Monk[1] **Manuel Pena**[2*] **Virginia Selgas**[2]

[1] Department of Mathematical Sciences, University of Delaware, U.S.A.
[2] Departamento de Matemática Aplicada I, Universidad de Vigo, Spain
[3] Departamento de Matemáticas, Universidad de Oviedo, Spain

ABSTRACT

The Trefftz Discontinuous Galerkin (TDG) method is a discontinuous Galerkin method where the set of basis functions used in each cell belongs to the nullspace of the differential operator. For example, for the Helmholtz equation in two dimensions, the set of basis functions can be chosen as a set of plane waves with different directions of propagation.

This is an interesting approach for problems with very high wavenumber, as much fewer basis functions are needed to approximate a given solution than if using a standard DG-FEM method where the basis functions are polynomials. However, in general, the condition number of the matrices appearing in the TDG method is much higher, and can affect the accuracy of the method.

In this work, we show results obtained when a waveguide with different scatterers is simulated. The radiating conditions are imposed via an approximation of the Neuman to Dirichlet map which allows us to reduce the number of cells in the mesh.

Keywords: *waveguide, Helmholtz equation, Neumann-to-Dirichlet map, Trefftz Discontinuous Galerkin.*

1. INTRODUCTION

In this work we have implemented a Trefftz discontinuous Galerkin method [1] to solve the Helmholtz equation in a two dimensional infinite waveguide. The accurate simulation of this problem for high wave numbers is challenging for traditional finite element methods. The use of Perfectly Matched Layers (PMLs) is problematic as there are evanescent modes as well as traveling ones.

For this reason we artificially cut the infinite waveguide at two sections (see Fig. 1) and impose radiating conditions on those boundaries. For non-absorving materials, the TDG is a generalization of the Ultra Weak Variation Formulation (see [2]).

2. THE MODEL

We will model a bounded section of an otherwise infinite waveguide, as:

$$\Omega := \left\{(x,y) \in \mathbb{R}^2 \,:\, -R < x < R,\, 0 < y < H\right\}. \quad (1)$$

The boundary of Ω consists of two parts. The walls of the waveguide:

$$\Gamma := (-L, L) \times \{0, H\}, \quad (2)$$

where a sound-hard condition is imposed; and the artificial boundaries:

$$\Sigma := \{-L, L\} \times (0, H), \quad (3)$$

where a non-reflecting condition based on the Neumann to Dirichlet operator (NtD) is imposed.

The total field u satisfies the Helmholtz equation in Ω except for the domain $\mathcal{D} \subset \Omega$ which models the presence of a sound-soft scatterer. The full model reads:

$$\begin{cases} \Delta u + k^2 u = 0 & \text{in } \Omega \setminus \overline{\mathcal{D}} \\ u = 0 & \text{on } \partial\mathcal{D} \\ \nabla u \cdot \mathbf{n} = 0 & \text{on } \Gamma \\ u - u^{\text{inc}} = \text{NtD}\left(\nabla u \cdot \mathbf{n} - \nabla u^{\text{inc}} \cdot \mathbf{n}\right) & \text{on } \Sigma \end{cases} \quad (4)$$

*Corresponding author: manuel.pena@uvigo.gal.

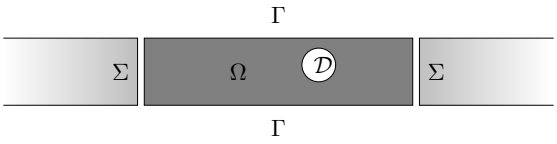

Figure 1. Representation of the computational domain Ω as well as its boundaries.

where $\mathbf{n}$ stands for the unit outward pointing normal and u^{inc} is a known incident field.

For the exact solution, the radiation condition is equivalent to using the more conventional Dirichlet to Neumann map, i.e.:

$$\nabla u \cdot \mathbf{n} - \nabla u^{\text{inc}} \cdot \mathbf{n} = \text{DtN}\left(u - u^{\text{inc}}\right). \tag{5}$$

We choose to use the Neumann to Dirichlet map as the discrete solution is only piecewise smooth.

2.1 Neumann to Dirichlet map

The Neumann to Dirichlet map is defined as:

$$\begin{aligned} \text{NtD}\colon \tilde{H}^{-1/2}(\Sigma) &\to H^{1/2}(\Sigma) \\ u &\mapsto \sum_{s=0}^{\infty} \frac{1}{i\beta_s} \int_0^H u(\eta)\theta_s(\eta)\,\mathrm{d}\eta\ \theta_s \end{aligned} \tag{6}$$

where $\tilde{H}^{-1/2}(\Sigma)$ is the dual space of

$$\tilde{H}^{1/2}(\Sigma) \coloneqq \left\{ v_{|\Sigma} :\ v \in H^{1/2}(\partial\Omega) \right\} \tag{7}$$

and $\{\theta_s\}$ is an orthonormal basis of harmonic functions on the interval $(0, H)$, that is:

$$\theta_s(y) = \sqrt{\frac{2}{H}} \cos\left(s\pi \frac{y}{H}\right), \quad s = 0, 1, \ldots \tag{8}$$

and β_s are the longitudinal wavenumbers:

$$\beta_s = \sqrt{k^2 - \left(\frac{s\pi}{H}\right)^2} \tag{9}$$

of the corresponding modes:

$$g_s^{\text{R}}(\mathbf{x}) = e^{i\beta_s x} \cos\left(s\pi \frac{y}{H}\right), \ g_s^{\text{L}}(\mathbf{x}) = e^{-i\beta_s x} \cos\left(s\pi \frac{y}{H}\right),$$

where the superscripts "L" and "R" stand for modes propagating (see Fig. 2) or exponentially decaying (see Fig. 3) towards the left or right, respectively.

Figure 2. Depiction of the real part for the fourth propagating mode.

Figure 3. Depiction of an evanescent mode. The colormap is capped to the maximum values inside the computational domain, i.e. the values at the left boundary.

It is worth mentioning that there are only a finite number of propagating modes, as for $s > \frac{kH}{\pi}$ all modes are evanescent. This allows for approximating the Neumann to Dirichlet map as a finite sum when implementing the numerical scheme.

3. DG-TREFFTZ METHODS

Let $\mathcal{T}_h$ denote a triangular mesh of the domain $\Omega \setminus \overline{\mathcal{D}}$ with diameter h. For each $K \in \mathcal{T}_h$ let

$$V(K) \coloneqq \left\{ v \in H^2(K) :\ \Delta v + k^2 v = 0 \right\}, \tag{10}$$

and the "broken" Trefftz space:

$$V(\mathcal{T}_h) \coloneqq \{ v \in L^2(\Omega \setminus \overline{\mathcal{D}}) :\ v|_K \in V(K)\, \forall K \in \mathcal{T}_h \}. \tag{11}$$

Functions in $V(\mathcal{T}_h)$ solve Eqn. (2) at each triangle K, however they are not smooth, in general, across its boundaries.

If we "test" that equation against a function $v \in V(\mathcal{T}_h)$ and integrate by parts twice we get:

$$\int_{\partial K} \left(\nabla u \cdot \mathbf{n}_K \overline{v} - u\overline{\nabla v \cdot \mathbf{n}_K}\right) \mathrm{d}\gamma = 0, \ \forall v \in V(K) \tag{12}$$

where $\mathbf{n}_K$ stands for the outward pointing normal with respect to triangle K. For every side E, given a normal vector $\mathbf{n}$, we define u^+ and u^- as the values at the boundary as:

$$u^{\pm}(\mathbf{x}) \coloneqq \lim_{\epsilon \to 0} u(\mathbf{x} \mp \epsilon \mathbf{n}) \tag{13}$$

This way, we can define the average and the normal jump:

$$\{\!\{u\}\!\} \coloneqq \frac{u^+ + u^-}{2}, \tag{14}$$

$$[\![u]\!]_{\mathbf{n}} \coloneqq u^+\mathbf{n} - u^-\mathbf{n}, \tag{15}$$

without taking into account the normal chosen.

Now, by adding across all the triangles in $\mathcal{T}_h$ we get a condition that enforcess the continuity across triangles:

$$\sum_{E\in\mathcal{E}_h^I}\int_E \left(u\,[\![\nabla\overline{v}]\!]_{\mathbf{n}} - \nabla u\cdot[\![\overline{v}]\!]_{\mathbf{n}}\right)\,d\gamma + \sum_{E\in\mathcal{E}_h\setminus\mathcal{E}_h^I}\int_E \left(u\nabla\overline{v}\cdot\mathbf{n} - \nabla u\cdot\mathbf{n}\,\overline{v}\right)\,\mathrm{d}\gamma = 0, \tag{16}$$

where $\mathcal{E}_h$ stands for the set of sides of the mesh (also known as the skeleton) and $\mathcal{E}_h^{\mathrm{I}} \subset \mathcal{E}_h$ for the inner ones.

3.1 Numerical fluxes

As it is done in conventional DG methods, the values of u and ∇u on the boundaries of the elements are replaced by numerical fluxes $\hat{u}$ and $ik\hat{\boldsymbol{\sigma}}$.

For an interior edge we set:

$$\begin{aligned}\hat{u} &= \{\!\{u\}\!\} + \frac{\mathfrak{b}}{ik}[\![\nabla_h u]\!]_{\mathbf{n}}\,,\\ ik\hat{\boldsymbol{\sigma}} &= \{\!\{\nabla u\}\!\} + i\mathfrak{a}k\,[\![u]\!]_{\mathbf{n}}\,.\end{aligned} \tag{17}$$

If the edge belongs to the walls of the waveguide we set:

$$\begin{aligned}\hat{u} &= u + \frac{\mathfrak{d}_1}{ik}\nabla u\cdot\mathbf{n},\\ ik\hat{\boldsymbol{\sigma}} &= \mathbf{0}.\end{aligned} \tag{18}$$

If the edge is on the boundary of the scatterer we set:

$$\begin{aligned}\hat{u} &= 0,\\ ik\hat{\boldsymbol{\sigma}} &= \nabla u + i\mathfrak{a}ku\boldsymbol{n}.\end{aligned} \tag{19}$$

And if it is on the artificial boundaries:

$$\begin{aligned}\hat{u} =& u^{\mathrm{inc}} + \mathrm{NtD}\left(\nabla u\cdot\mathbf{n} - \nabla u^{\mathrm{inc}}\cdot\mathbf{n}\right) +\\ & -ik\mathfrak{d}_2\mathrm{NtD}^*\left(\mathrm{NtD}\left(\nabla\left(u-u^{\mathrm{inc}}\right)\cdot\mathbf{n}\right) - u + u^{\mathrm{inc}}\right),\\ ik\hat{\boldsymbol{\sigma}} =& \nabla u +\\ & -ik\mathfrak{d}_2\left(\mathrm{NtD}\left(\nabla\left(u-u^{\mathrm{inc}}\right)\cdot\mathbf{n}\right) - u + u^{\mathrm{inc}}\right),\end{aligned} \tag{20}$$

where $\mathrm{NtD}^* : L^2(\Sigma) \to L^2(\Sigma)$ is the adjoint of the NtD map and $\mathfrak{a}$, $\mathfrak{b}$, $\mathfrak{d}_1$, and $\mathfrak{d}_2$ are tunable parameters that can control the stability of the scheme. For the particular case of $\mathfrak{a} = \mathfrak{b} = \mathfrak{d}_1 = \mathfrak{d}_2 = 1/2$ we recover the UWVF except for the artificial boundaries (see [2]).

4. VARIATIONAL FORMULATION

After substitution of the numerical fluxes in Eqn. (16) we get that the discrete solution $u_h \in V(\mathcal{T}_h)$ must satisfy:

$$a_h(u_h, v_h) = \ell_h(v_h) \quad \forall v_h \in V_h(\mathcal{T}_h), \tag{21}$$

where $a_h : V(\mathcal{T}_h)\times V(\mathcal{T}_h) \to \mathbb{C}$ is the sesquilinear form:

$$\begin{aligned}a_h(w,v) =& \sum_{E\in\mathcal{E}_h^I}\int_E \left(\{\!\{w\}\!\} + \frac{\mathfrak{b}}{ik}[\![\nabla w]\!]_{\mathbf{n}}\right)\overline{[\![\nabla v]\!]_{\mathbf{n}}}\,d\gamma\\ & - \sum_{E\in\mathcal{E}_h^I}\int_E \left(\mathfrak{a}ik\,[\![w]\!]_{\mathbf{n}} + \{\!\{\nabla w\}\!\}\right)\overline{[\![v]\!]_{\mathbf{n}}}\,d\gamma\\ & - \sum_{E\in\partial\mathcal{D}}\int_E \left(\nabla u\cdot\mathbf{n} + \mathfrak{a}iku\right)\overline{v}\,\mathrm{d}\gamma\\ & + \sum_{E\in\Gamma}\int_E \left(w + \frac{\mathfrak{d}_1}{ik}\nabla_h w\cdot\mathbf{n}\right)\nabla\overline{v}\cdot\mathbf{n}\,d\gamma\\ & + \sum_{E\in\Sigma}\int_E \left(\mathrm{NtD}(\nabla w\cdot\mathbf{n})\nabla\overline{v}\cdot\mathbf{n} - \nabla w\cdot\mathbf{n}\,\overline{v}\right)\,\mathrm{d}\gamma\\ & - \sum_{E\in\Sigma}\int_E \mathfrak{d}_2 ik\left(\mathrm{NtD}(\nabla w\cdot\mathbf{n}) - w\right)\overline{\left((\mathrm{NtD}(\nabla v\cdot\mathbf{n}) - v\right)}\,\mathrm{d}\gamma\end{aligned} \tag{22}$$

and $\ell_h : V(\mathcal{T}_h) \to \mathbb{C}$ is the antilinear form:

$$\begin{aligned}\ell_h(v) =& \sum_{E\in\Sigma}\int_E \left(\mathrm{NtD}(\nabla u^{\mathrm{inc}}\cdot\mathbf{n}) - u^{\mathrm{inc}}\right)\overline{\nabla v\cdot\mathbf{n}}\,\mathrm{d}\gamma\\ & - \sum_{E\in\Sigma}\int_E \mathfrak{d}_2 ik\left(\mathrm{NtD}(\nabla u^{\mathrm{inc}}\cdot\mathbf{n}) - u^{\mathrm{inc}}\right)\overline{\left(\mathrm{NtD}(\nabla v\cdot\mathbf{n}) - v\right)}\,\mathrm{d}\gamma\,.\end{aligned} \tag{23}$$

5. PLANE WAVE CONVERGENCE

In this work we approximate $V(K)$ as a finite combination of plane waves, i.e. $V_p(K) \coloneqq \langle\varphi_j^K\rangle_{j=1}^{N_p}$ where the plane waves:

$$\varphi_j^K(\mathbf{x}) = e^{ik\mathbf{d}_j\cdot\mathbf{x}}, \quad j = 1,\dots,N_p = 2p+1$$

have propagating directions $\{\mathbf{d}_j\}$ linearly spaced in $\mathbb{S}^1$.

For this case we have proved the following estimates. If $u \in V(\mathcal{T}_h)\cap H^{s+1}(\Omega\setminus\overline{\mathcal{D}})$ for some $1 \le s \le \frac{p-1}{2}$, then:

- For fixed number of plane waves, N_p:

$$\|u - u_h\| \le Ch^{s-1}\left\|u^{\mathrm{inc}}\right\| \tag{24}$$

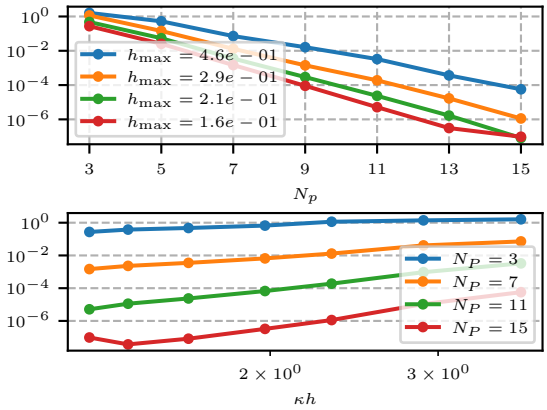

Figure 4. Relative error $\frac{\|u_h - u\|}{\|u\|}$ when u^{inc} is the first propagating mode.

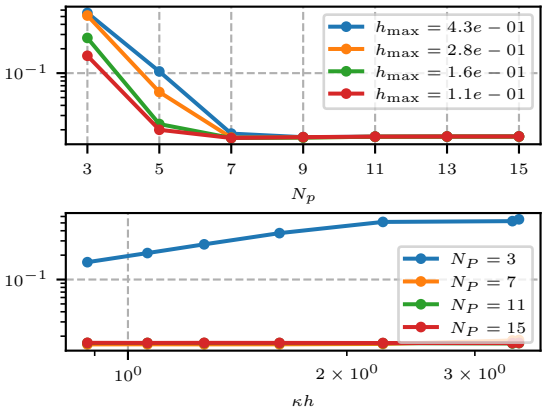

Figure 5. Relative error $\frac{\|u_h - u\|}{\|u\|}$ when using as Dirichlet data a point source located inside the scatterer.

- And for a fixed mesh diameter, h:

$$\|u - u_h\| \leq C_h \left(\frac{\log(p+2)}{p}\right)^{s-\frac{1}{2}} \|u^{\text{inc}}\| \quad (25)$$

where $\|\cdot\|$ stands for the L^2 norm in $\Omega \setminus \overline{\mathcal{D}}$.

In particular, for $u \in C^\infty\left(\Omega \setminus \overline{\mathcal{D}}\right)$ the method has faster than polynomial convergence in both p and h.

6. NUMERICAL TESTS

We show now numerical examples of the h and p convergence curves. Due to the lack of exact solutions when a scatterer is present, we only show two numerical tests: one where u^{inc} is a propagating mode with no scatterer, and one where the a point source located at $\mathbf{s} \in \mathcal{D}$:

$$G(\mathbf{x}, \mathbf{s}) := -\sum_{n=0}^{\infty} \frac{e^{i\beta_n |x - s_x|}}{2i\beta_n} \theta_n(s_y)\, \theta_n(y), \ \mathbf{x} \in \Omega \setminus \overline{\mathcal{D}}, \quad (26)$$

is used as Dirichlet data on the boundary of the scatterer.

In Fig. 4 we show the convergence results for a propagating mode when using $\mathfrak{a} = \mathfrak{b} = \mathfrak{d}_1 = \mathfrak{d}_2 = \frac{1}{2}$.

At the combination of the highest number of plane waves N_p and the smallest element diameter h we can see the onset of numerical instabilities due to the poor conditioning of the matrix.

In Fig. 5 we show the p and h convergence when testing the method with Dirichlet data on the scatterer corresponding to a point source located inside the scatterer. The convergence stalls earlier likely due to errors in the approximation of the exact solution (see Eqn. (26)) as a finite sum.

7. FUNDING

The research of the second author was partially supported by MICINN/AE/doi 10.13039/501100011033 grant PID2023-147790OB-I00 and by a Margarita Salas grant from the Ministerio de Universidades (RD 289/2021) funded by the European Union-NextGenerationEU. The research of the third author was partially supported MICINN grant PID2020-116287GB-I00.

8. REFERENCES

[1] R. Hiptmair, A. Moiola, and I. Perugia, "A survey of Trefftz methods for the Helmholtz equation," in *Building Bridges: Connections and Challenges in Modern Approaches to Numerical Partial Differential Equations* (G. R. Barrenechea, A. Cangiani, and E. H. Georgoulis, eds.), vol. 114 of *Lecture Notes in Computational Science and Engineering (LNCSE)*, pp. 237–278, Springer, 2016.

[2] C. J. Gittelson, R. Hiptmair, and I. Perugia, "Plane wave discontinuous Galerkin methods: analysis of the h-version," *Math. Model. Numer. Anal.*, vol. 43, pp. 297–331, 2009.